# Nanoscale

Accepted Manuscript


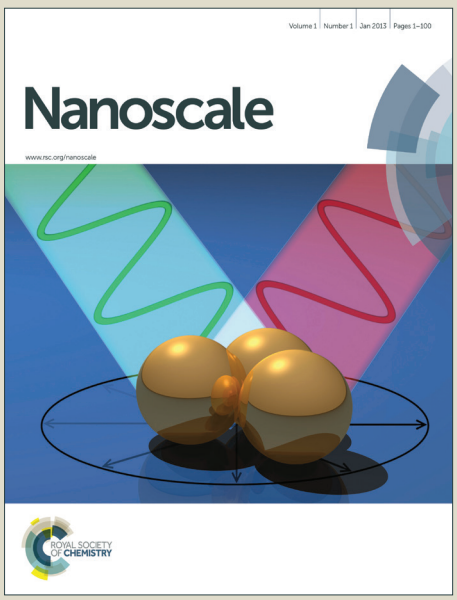





ROYAL SOCIETY OF CHEMISTRY

www.rsc.org/nanoscale

Journal Name

RSCPublishing

ARTICLE

# Kinetic Effects in the Photomediated Synthesis of Silver Nanodecahedra and Nanoprisms: Combined Effect of Wavelength and Temperature

Cite this: DOI: 10.1039/xoxxoooooox

Received ooth January 2012,
Accepted ooth January 2012

DOI: 10.1039/xoxxoooooox

www.rsc.org/

Haitao Wang, [a] Xiaoqiang Cui *,[a] Weiming Guan, [b] Xianliang Zheng, [a] Hetong Zhao, [a] Zhao Wang, [a] Qiyu Wang, [a] Tianyu Xue, [a] Chang Liu, [a] David J. Singh [a,c] and Weitao Zheng * [a]

Photomediated synthesis is a reliable, high yield method for the production of a variety of morphologies of silver nanoparticles. Here, we report synthesis of silver nanoprisms and nanodecahedra with tunable sizes via control of the reaction temperature and the irradiation wavelength. The results show that shorter excitation wavelengths and lower reaction temperatures result in high yields of nanodecahedra, while longer excitation wavelengths and higher reaction temperatures result in the formation of nanoprisms. The mechanism for the growth condition dependent evolution in the morphology of the silver particles is discussed as a kinetically controlled process. This is based on analysis of the reaction kinetics at various excitation wavelengths and temperatures. The energy barrier for the transformation from seeds to nanodecahedra is relatively high and requires a shorter wavelength. Thus longer wavelength illumination leads to the formation of nanoprisms. Thermodynamically stable five-fold twinning structures are shown to evolve from twin plane structures. The fast reaction rate at higher temperature favors the growth of nanoprisms by preferential Ag deposition on planar structures in a kinetics-controlled mode, while slower rates yield thermodynamically favored nanodecahedra.



## Introduction

The past decade has witnessed major strides in the development of methods for synthesizing and controlling the sizes and shapes of silver nanoparticles.[1-6] These nanoparticles have unique physical and chemical properties different from bulk materials.[7-9] This progress has been enabling for the wide use of silver nanomaterials in the fields of catalysis,[10-11] optical systems,[7, 12-15] drug delivery,[16-17] photothermal therapy,[4] sensing,[18-19] and surface-enhanced Raman scattering (SERS).[20-23] Applications require defined properties and therefore control is of great importance in synthesis. In this regard, photomediated methods, pioneered by Mirkin and coworkers, have proven to be very effective for making anisotropic silver nanoparticles with controllable sizes and shapes.[6, 24-25] Small spherical silver nanoparticles can be selectively converted into triangular nanoprisms by irradiating solutions containing trisodium citrate and bis(p-sulfonatophenyl)phenylphosphine dipotassium salt (BSPP) with light of appropriate wavelengths.[6] Mechanistic studies of this reaction have shown that the photomediated process is driven by silver redox cycles involving reduction of silver cations by citrate on the silver particle surface and oxidative dissolution of small silver particles by $O_2$.[26]

There is a substantial body of work on controlling the shape and size of silver nanoparticles by adjusting the wavelength,[6, 27-28] capping agents[29] and pH[30] in photomediated synthesis. However, the role of temperature has been less studied. We recently found that temperature affects not only the rate and yield, but also the morphology of silver nanoparticles in a system where we irradiated with sodium lamps.[31] An interesting transformation process was observed at a lower temperature of 20 °C: silver nanoprisms grew first and then subsequently completely transformed into nanodecahedra. However, the influence of the irradiating wavelength was not studied and the intrinsic mechanism underlying this observation remained unclear.

To address these questions, we designed and built a system consisting of a temperature controlled water-filled tank and well-fitted light-emitting diode (LED) arrays. The irradiation wavelength is then controlled with a narrow-band emission (±5 nm) in addition to control of the reaction temperature in the photomediated synthesis (Fig. S1). Remarkably, we find that

both nanoprisms and nanodecahedra can be controllably synthesized by adjusting the temperature under shorter wavelength irradiation; but that nanoprisms are the sole product independent of reaction temperature with a longer irradiation wavelength of 590 nm. This is an unexpected result in the context of prior work and suggests that the mechanism for growth may be richer than previously anticipated. Based on the observations, we propose a growth mechanism consisting of a primary step and a secondary step. The results provide the first indication that there is a primary step that is affected by the wavelength, presumably corresponding to the excitation energy required for the transformation from seeds to nanodecahedra or nanoprisms, and a secondary step affected by the temperature, presumably leading to a competition between kinetics and thermodynamics in the process. Kinetics is therefore important in determining the products.

## Results and discussion.

### Time Dependent UV-vis Spectra at Various Irradiation Wavelengths and Reaction Temperatures.

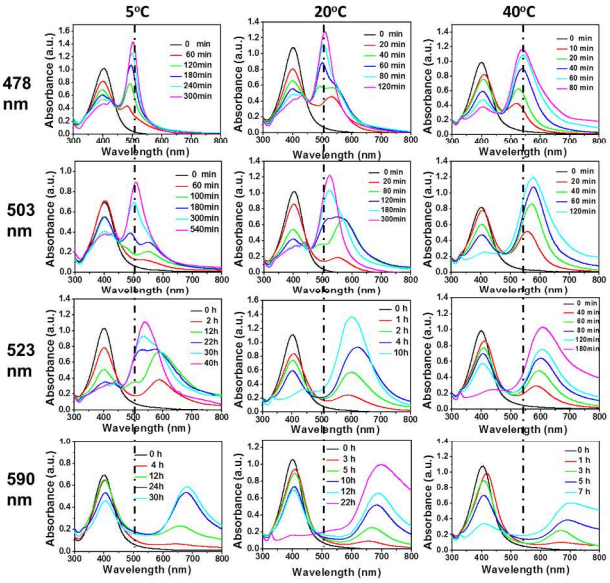


**Fig. 1** Time evolution of UV-vis absorbance spectra of silver colloids synthesized at various irradiation wavelengths (478 nm, 503 nm, 523 nm, and 590 nm) and reaction temperatures (5 ºC, 20 ºC, and 40 ºC).

The morphological evolution of silver nanoparticles synthesized at various irradiation wavelengths (478, 503, 523, and 590 nm) and reaction temperatures (5, 10, 20, 30, and 40 ºC) was monitored by UV-vis spectra (Fig. 1 and S3). The original peak at 400 nm in all the spectra is characteristic of spherical seeds,[5] most of which are small single crystals or multi-twinned particles with the average sizes of 4.7 ± 0.3 nm (Fig. S2). When the silver colloid was irradiated by 478 nm LED illumination at 5 ºC, the 400 nm band showed a decrease in intensity, concomitant with a slight increase at around 480 nm. In the next few minutes, the band at 480 nm showed a gradual increase that should be ascribed to the formation of silver nanodecahedra.[32] The intensity of this new band increased considerably on further irradiation and red-shifted to ca. 500 nm, accompanied by a concomitant decrease in intensity of the 400 nm band with an isosbestic point at 440 nm. This indicates the transformation of silver nanoseeds into silver nanodecahedra.

We observe a considerably different behavior in the UV-vis spectra when we use a higher reaction temperature of 20 ºC. The peak at 530 nm grows significantly in the early stage of synthesis within 20 min. Another new band appears at 490 nm and increases in intensity with further exposure, becoming very prominent at 40 min. Finally, the peak at 530 nm disappears and the peak at 490 nm red-shifts to ca. 510 nm. This phenomenon is consistent with our previous report where it was shown this behavior can be ascribed to the transformation from nanoprisms to nanodecahedra.[31] The 400 nm band showed a decrease and red shifted slightly in the first 10 min at 40 °C, owing to growth in size of the silver seeds.[32] The reaction is fast and only an increase of new wider band around 540 nm is observed, concomitant with the appearance of a tailing peak on its long wavelength side, indicating a mixture was obtained.[31-32] Further irradiation caused a red shift of the band position, which can be ascribed to a size increase of nanoparticles.[6] Transformation from nanoprisms to nanodecahedra does not occur at 40 °C. The spectral changes seen with 503 nm irradiation at 5 °C are similar to those obtained with 478 nm excitation at 10 or 20 °C. This means that the transformation from nanoprisms to nanodecahedra occurred under these conditions.

Irradiation with 523 nm light also results in an analogous transformation behavior at 5 and 10 °C and no transformation at temperatures of 20, 30, or 40 °C. An interesting result that is worthy of note is that the final products were nanoprisms at all temperatures (5-40 °C) with 590 nm LEDs irradiation. The spectra obtained at 10 °C and 30 °C are shown in Fig.S3.

Thus the particle growth process and products are dependent on the irradiation wavelength, almost certainly due to the role of surface plasmon excitations. We note that the electromagnetic field intensity can be greatly enhanced in the region between nearby particles, leading either to fusion of particles in an edge-selective manner or to the growth of the particles until they reach their light controlled final size, as discussed previously.[5-6, 33] Here we have shown that silver nanoparticles with tunable surface plasmon resonance properties can be prepared with control via changes in the excitation wavelengths and temperatures. Therefore there must be a relationship between the excitation wavelength and the corresponding SPR absorption band of the prepared nanoparticles at different reaction temperatures.[24] The positions of SPR absorption bands for each irradiation wavelength have been examined and are plotted in Fig. S4. In general, there is an approximate linear correlation between the excitation wavelength and the SPR peaks. It is worthy of noting that the longer the irradiation wavelength, the SPR becomes more red-shifted. The SPR peak of final product is always longer than the irradiation wavelength, [34-35] which implies that the energy of excitation must be higher than the SPR energy of products. The curve obtained at 20 ºC exhibits an exceptional trend that should be attributed to different morphologies at various excitation wavelengths: 478 and 503 nm excitation produces nanodecahedra; while 523 or 590 nm excitation produces nanoprisms. This result strongly indicates that the formation of the nanoparticles is a plasmon-mediated process.[2]

### Temperature Effect on Morphology.

TEM images were used to confirm the morphologies of Ag nanoparticles that are described in the discussion of the UV−vis spectra above. Fig. 2 shows results for the final products synthesized using 503 nm LED irradiation at different temperatures. Most of the nanoparticles in the image are decahedral in shape for growth at 10 and 20 ºC. However, a mixture of shapes of nanodecahedra and nanoprisms can be

observed at the higher growth temperature of 30 °C; nanoprisms are formed at the still higher temperature of 40 °C. It can be concluded the morphology of the final products is strongly dependent on the reaction temperature. The mean edge length of the nanodecahedra synthesized with 478 nm LED irradiation increased as the reaction temperature increased (Fig. S5). At reaction temperatures of 5, 10, 20, 30, and 40 ºC, the average edge lengths of the nanodecahedra are 22.8 ± 3.5, 31.1 ± 6.9, 37.5 ± 8.9, 45.0 ± 9.2, and 49.1 ± 9.8 nm, respectively. It seems that an increasing reaction temperature promotes the deposition silver atoms on the surface. This result is consistent with our previous report.[31]

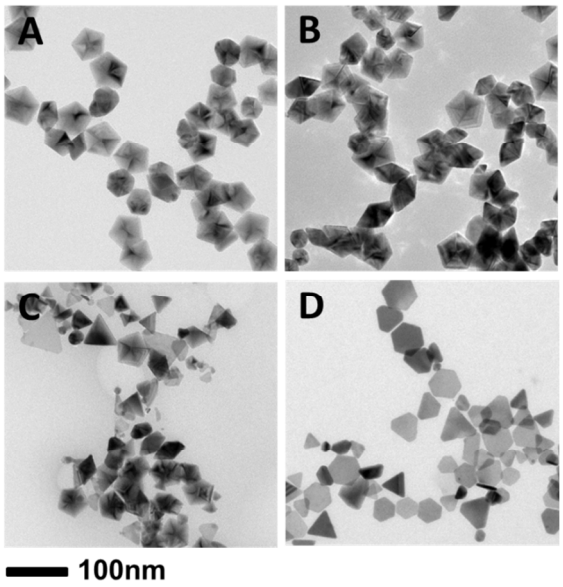


**Fig. 2** TEM images of final silver nanoparticles synthesized with 503 nm LED irradiation at different reaction temperatures: (A) 10 ºC, (B) 20 ºC, (C) 30 ºC, (D) 40 ºC. (Scale bars: 100nm)

**Wavelength Effect on Morphology.**

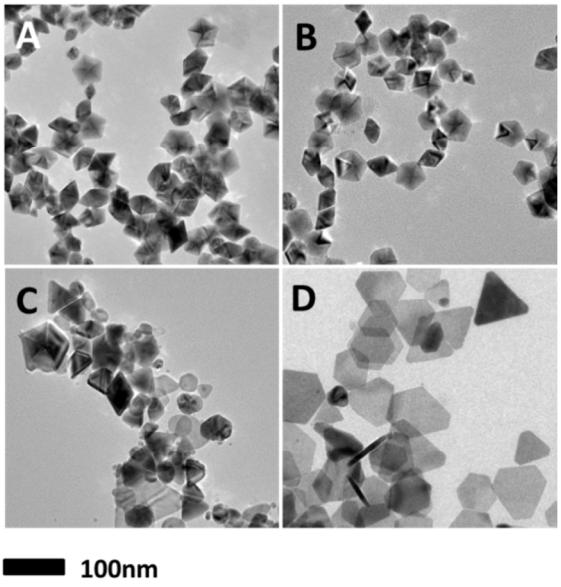


**Fig. 3** TEM images of the final products synthesized at 10 ºC under the corresponding LED irradiation at the different wavelengths: (A) 478 nm; (B) 503 nm; (C) 523 nm; (D) 590 nm.

As mentioned, one of our main goals was to investigate the effect of wavelength on the synthesis. Fig. 3 shows the resulting final products synthesized at 10 °C with the LED irradiation at 478, 503, 523, and 590 nm. As shown, the products are nanodecahedra with irradiation at 478 and 503 nm, nanoprisms with 590 nm irradiation, and a mixture of these morphologies with 523 nm irradiation. The TEM images of the final products synthesized at 5, 20, 30, and 40 °C are also displayed in Fig. S6-S9. It can be concluded that the wavelength plays an essential effect on morphology of the final products.

**Summary of Products at Different Wavelengths and Reaction Temperatures.**

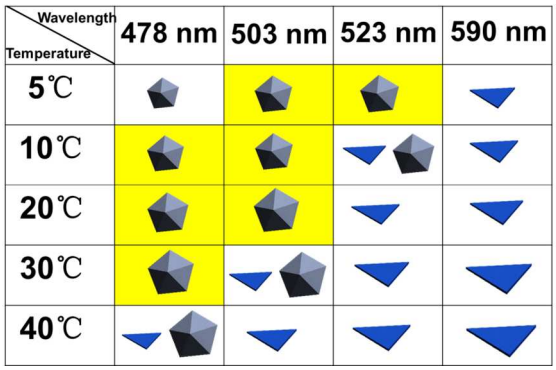


**Fig. 4** A summary of the relationship between photomediated reaction conditions and resulting product morphologies. (Yellow background: transformation from nanoprisms to nanodecahedra)

Fig. 4 shows a summary of the products obtained based on the UV–vis spectra and TEM, at four wavelengths (478, 503, 523, and 590 nm) and five reaction temperatures (5, 10, 20, 30, and 40 °C). The morphologies of the final products strongly depend on these parameters with specific conditions yielding nanodecahedra, nanoprisms or mixtures. As shown in the upper-left part of the chart a shorter wavelength (478 nm) and lower reaction temperature (5 °C) yields nanodecahedra by direct growth from small pentagon-like particles. The yellow background part of the chart illustrates the fact that with longer wavelength and higher reaction temperature, silver nanoprisms are grown at first, and then fully transformed into nanodecahedra (based on the time evolution of the spectra). As shown on the bottom-right, only nanoprisms are obtained at even longer wavelength and higher reaction temperature. Mixtures of nanodecahedra and nanoprisms were obtained in the boundary region. Thus a shorter excitation wavelength and lower reaction temperature is necessary to synthesize nanodecahedra with high yield; while a longer excitation wavelength and higher reaction temperature results in the formation of nanoprisms.

**Morphology evolution.**

The distinct evolution of the spectra at various excitation wavelengths and reaction temperatures, discussed above, suggests different growth pathways of silver nanostructures. We took time-dependent TEM images to study the morphological evolution with 478 nm LED irradiation at 5, 20, and 40 °C, as shown in Fig. 5 and 6. Fig. 5A (5 °C after 20 min) shows quasi-spherical seeds and five-fold twined pentagon-like particles. The particles with irregular

shape in the image may be attributed to the coalescence of smaller particles.[34] Fig. 5B and 5C show TEM images of the silver nanoparticles at 60 and 300 min, respectively. Most of the quasi-spherical seeds transform into decahedral silver nanoparticles gradually corresponding to the observed decrease of the plasmon band intensity at 400 nm and the increase of the plasmon band intensity at 500 nm in Fig. 1. The size of silver nanodecahedra increased from 18.5 ± 2.5 nm at 60 min to 22.8 ± 3.5 nm at 300 min (Fig. S10), accompanied by the vanishing of small silver seeds due to Ostwald ripening[35] . TEM images of synthesized silver colloids at 40 °C at 20, 40, and 80 min are shown in Fig. 5 D-F. These images show that silver platelets are formed at 20 min and that with further irradiation a mixture of nanoprisms, with minor fractions of nanodecahedra and small particles are present. After 80 min irradiation, most of the edges of the silver nanoparticles are seen to be irregularly etched, resulting from the thermal effect.[36] The results indicate that the transformation from nanoprisms to nanodecahedra will not happen at 40 °C consistent with the results shown in Fig. 1, where only one peak is observed.

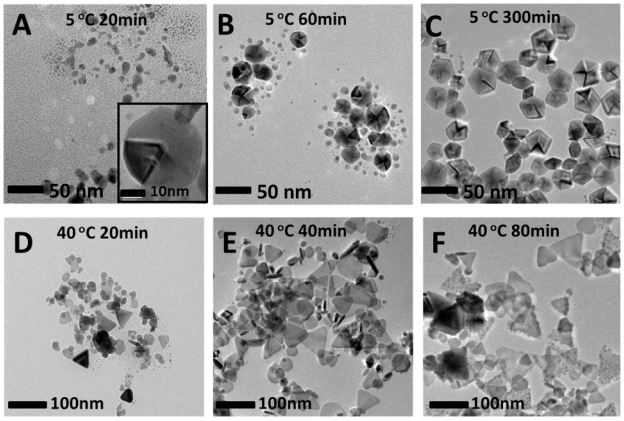


**Fig. 5** TEM images of silver nanoparticles synthesized with 478 nm LED irradiation at 5 ºC and 40 ºC at different reaction time.

Returning to Fig. 1, the UV-vis spectra in the different panels at 20 °C show considerable variations with the irradiation wavelength. To analyze these, the spectral peaks between 300 and 800 nm were fitted with three Gaussian functions. An example of the fits obtained is shown for the spectrum with 478 nm LED irradiation of 40 min at 20 °C in Fig. 6A. A similar fitting procedure was carried out for the absorption spectra at other irradiation wavelengths and reaction temperatures. Fig. 6B displays the evolution of corresponding absorbance percentages ascribed to seeds, prisms, and decahedra. This shows the correlation of the peak intensity due to nanoprisms with that for nanodecahedra. Fig. 6C-F shows the TEM images taken at different stages of the photomediated growth process. The seeds developed into prisms with irradiation for 20 min. With further exposure, the nanoprisms vanished and are transformed into nanodecahedra. All silver nanoprisms were finally transformed into nanodecahedra under continued irradiation for 120 min at 20 °C.

**Photomediated Reaction Kinetics.**

Kinetic curves were obtained from Fig. 1 to extract the shape evolution of the silver nanoparticles during growth. This was done by plotting results of the fits with Gaussian functions. The absorbance percentages due to seeds, nanoprisms, and nanodecahedra during 503 nm LED irradiation as estimated from the fits are shown in Fig. 7. The temperature effects on the reaction rate were obtained from the absorption intensities of silver seeds, nanoprisms and nanodecahedra. The seed concentration decreases with reaction time, and the consumption rate increases with increasing of the temperature. Two distinctive stages can be identified in the reaction process. Silver nanoprisms grow first at all reaction temperatures (Stage I), but decrease at 5 °C, 10 °C, and 20 °C (Stage Ⅱ). The formation rate of nanodecahedra is slow at Stage Ⅰ, and a sudden increase can be observed at 5 °C, 10 °C, and 20 °C at Stage Ⅱ, implying that a transformation from nanoprisms to nanodecahedra occurrs. No nanodecahedra formation is found at 40 °C (Stage Ⅱ). The reaction terminates once the silver seeds and small nanoclusters are consumed.[5] This result indicates that higher temperatures lead to faster reaction rates.

Irradiation wavelength also clearly affects the reaction rate. The kinetic curves obtained at other excitation wavelengths of 478, 523, and 590 nm exhibit a similar trend as shown in Fig. S11-S13. Higher energy excitation (shorter wavelength) leads to faster reaction rates. Silver nanoprisms became the sole products at five temperatures of 5, 10, 20, 30, and 40 °C with 590 nm irradiation. The time dependent decrease in the absorbance from the seeds at different irradiation wavelengths and reaction temperatures was investigated (Fig. S14). In general, the reaction rate at a fixed reaction temperature with shorter wavelength irradiation is faster than that for longer wavelength irradiation. Thus shorter, higher energy excitation wavelengths lead to faster rates of reaction.[22]

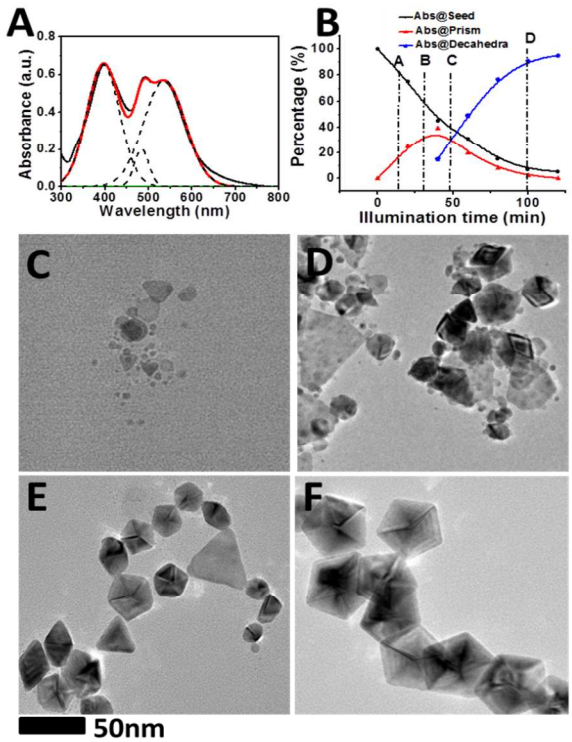


**Fig. 6** (A) UV-vis spectrum of silver nanoparticles obtained by 478 nm LED irradiation for 40 min at 20 ºC. The result from fitting with three Gaussian functions is indicated by the dash lines. (B) Corresponding absorbance percentages of seeds, prisms, and decahedra as a function of illumination time. TEM images of silver nanoparticles synthesized with 478 nm LED irradiation at 20 ºC at different reaction time：(C) 20 min, (D) 40 min, (E) 60 min and (F) 120 min. (Scale bar: 50 nm)

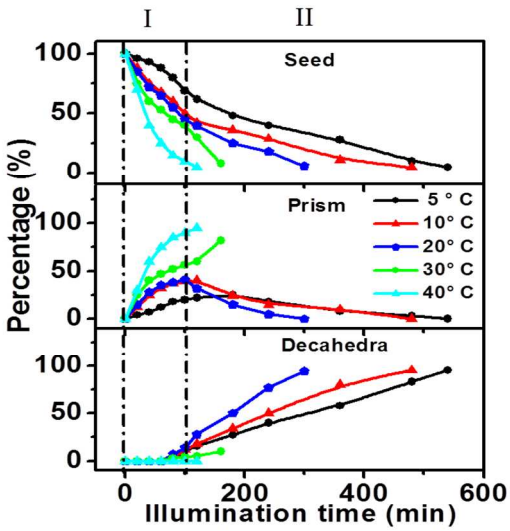


**Fig. 7** Corresponding absorbance percentages of seeds, prisms, and decahedra during 503 nm LED irradiation at different reaction temperatures as a function of illumination time.

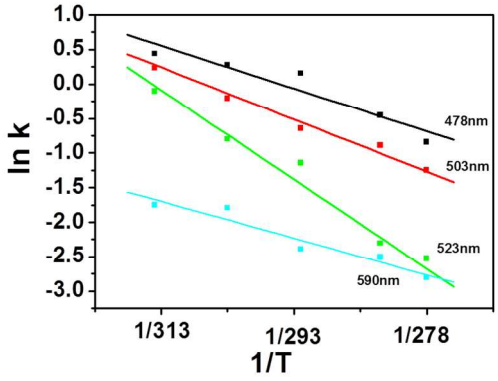


**Fig. 8** Arrhenius plots obtained at various irradiation wavelengths, lnk vs 1/T.

Based on the above a two-step mechanism is proposed, namely, primary process and secondary process, as shown in equation (1)-(3) in the Supporting Information. Nanoparticles in the ground state can be excited by any oscillating electric field of an appropriate frequency.[33] The silver nanoparticles thus absorb photons and enter short lived excited states (denoted Ag*), specifically states characterized by excitation of plasmon transitions in the primary process.[33] As noted previously, excitation of plasmon transitions could enhance the generation of excited states in the immediate vicinity of the nanoparticle, affecting electron- and hole-transfer processes that can readily participate in photoredox processes.[33, 37] The secondary process corresponding to the chemical reaction of silver cation reduction can be analyzed by an Arrhenius equation. Plasmon excitations are charge excitations and therefore these imply ultrafast charge separation on the nanoparticle surface. This likely leads to face-selective silver cation reduction, and thus anisotropic crystal growth.[37] During this process, silver nanoparticles growth usually involves rapid reduction of silver ion precursors on various crystalline faces through a thermal process. The reaction rate (k) is thus expressed as follows:

$$k = Ae^{-Ea/RT},$$

or $$\ln k = -Ea/RT + \ln A,$$

where A is the pre-exponential factor, Ea is the apparent activation energy, R is the ideal gas constant, and T is the absolute temperature (in kelvin). Rate constants (k) were obtained by plotting the decreasing concentration of the reactant (absorption of Ag seeds) versus reaction time (details in supporting information, Fig. S15-S18) wavelengths are shown in Fig. 8. It can be seen that lnk is approximately linear with 1/T.

The Arrhenius parameters for this reaction such as pre-exponential factor (A), and activation energy are presented in Table S1. The value of obtained activation energy and pre-exponential factor increases as the irradiation wavelength increases from 478 nm to 523 nm. This may be attributed to a situation where more silver nanoparticles are excited to the excited-state with shorter wavelength irradiation perhaps due to the higher energy in primary process. Then the silver nanoparticles excited at shorter wavelength may need lower activation energy in the secondary process. With 590 nm irradiation the silver nanoparticles obtain less excitation energy. The results can then be rationalized in a model where nanoprisms need lower activation energy for the secondary process.

**Mechanism: Kinetics and Thermodynamics.**

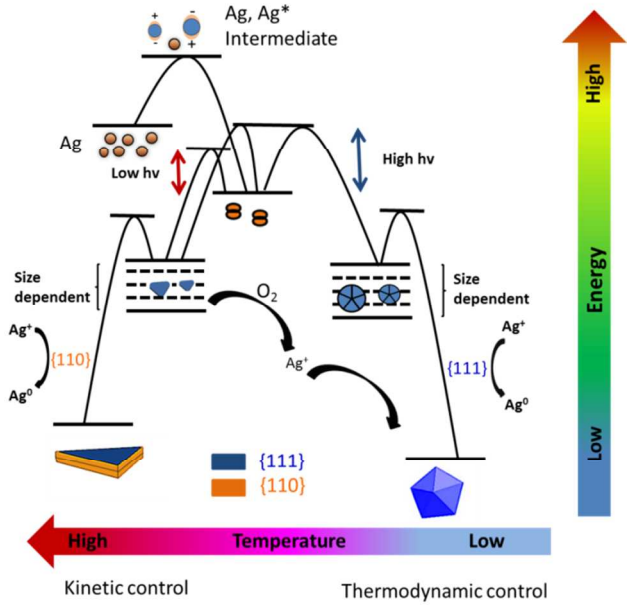


**Fig. 9** Schematic illustration of the growth pathway in photomediated synthesis of silver nanodecahedra and nanoprisms.

The results described above indicate that the growth pathway changes over the course of the reaction (Fig. 9) and can be understood as follows. Under irradiation, silver nanoparticles enter short lived excited states Ag* intermediate and then aggregate into planar twining seeds.[26,33] The planar twining seeds are competitively transformed into small silver nanoprisms or five-fold twinning seeds. The energy barrier for conversion is provided by plasmon excitation by irradiation light.[25] The required excitation energy for the formation of decahedra in primary process is relatively high.[37, 40]

Thus at longer wavelength, the lower resulting excitation energies (low hv indicated by red arrow) are not able to efficiently overcome the energy barrier for conversion of planar structure seeds to five-fold twinning seeds, so nanoprisms were the sole products with 590 nm irradiation even at lower reaction temperature. At short wavelength, the high excitation energies (high hv indicated by blue arrow) are able to overcome the both energy barriers for planar and five-fold twinning seeds, thus both nanoprisms and nanodecahedra can be formed. The energy of nanoprisms and nanodecahedra varies during the reaction since it is size dependent.[37] Alternatively, $Ag^+$ ions may be selectively reduced on different faces, which leads to subsequent different selective deposition rates for Ag on various faces.[39] Growth on {110} facets occurs and results in the formation of nanoprisms, while {111} deposition results in the formation of nanodecahedra. The addition of single Ag atoms may therefore be kinetically suppressed on {111} facets, resulting in higher excitation barriers for nanodecahedra. Planar structure seeds grow quickly under kinetic control and this leads to the formation of nanoprisms. The peak from nanoprisms appears early in the kinetic curve (Figure 7, S11-13); five-fold twinned seeds are more likely to be produced under thermodynamic control – i.e. they are thermodynamically but not kinetically favored. This results in the formation of nanodecahedra at low reaction temperatures with slow reaction rates (478 nm irradiation at 5 ºC). A competition between the kinetics and thermodynamics controls the process at intermediate conditions – nanoprisms form at first, favored by kinetics, and then the transformation from nanoprisms to nanodecahedra occurs under thermodynamic control, owing to the lower energy of nanodecahedra.[37, 41] This is consistent with UV-vis spectra and kinetic curves.

Mirkin and co-workers have demonstrated that the growth of a single stable twin plane can induce the growth of additional twin planes such as a five-fold twinning plane.[25] We verified the planar structure silver nanoparticles can transformed to five-fold twinning particles under appropriate conditions, but it is irreversible (Fig. S19). Silver nanodecahdra or nanoprisms were found to be stable at large sizes. This is not reversible by changing the reaction conditions (Fig. S20). This should be attributed to low chemical potential energy.[37, 40] We conducted a set of experiments based on kinetic control growth to validate the proposed mechanisms and verified that the platelet structure and five-fold twinning structures seeds formed in the photomediated synthesis, but not exist in the as-prepared seed (Fig. S21). Silver nanodecahedra are more stable than nanoprisms, owing to the lower energy of nanodecahedra[41] (Fig. S22, S23).

We also investigated the effect of changing the light intensity. The as-prepared seeds were irradiated with a wavelength of 478 nm at 40 °C using filters with various transmittances of 15%, 25%, 70%, and 100% (100% corresponds to a power of 1.6 $mW/cm^2$, i.e. the results described in the above paragraphs). The reaction rate increased with increasing intensity as expected. The products obtained at various intensities were mixtures of silver nanoprisms and nanodecahedra (Fig. S24, S25). The reaction rate at 40 °C with a filter transmittance of 15% decrease to a value similar to that obtained at 5 °C with 100% transmittance (no filter). The products were then a mixture of silver nanoprisms and nanodecahedra (Fig. S26). When the intensity was decreased, the formation rates of both nanoprisms and nanodecahedra decreased. It should be point out that the diffusion rate and concentration could be influenced by the reaction temperature.[42] So we conducted experiments to investigate the role that the concentration of reactants plays in the kinetic process. The results suggest that both increasing the reaction temperature and the concentration of reactants can improve the reaction rate (Fig. S27). It can be seen that increasing the concentration of reactants can change the products similar to the effect of increasing the reaction temperature. Silver nanodecahedra were the final products favored by the thermodynamic control. The results suggest that both increasing the concentration of reactants and light intensity can improve the reaction rate, but similar products can be obtained. This suggested that the transformation process that controls the final morphology and involves a competition between the kinetics and the thermodynamics is governed by reaction temperature. Silver nanodecahedra were the final products favored by thermodynamic control at lower temperatures.

## Experimental Section

**Materials:** $AgNO_3$ (99.8%) was obtained from Shanghai Reagent NO.1 Plant. $NaBH_4$ (96.0%) was obtained from Sinopharm Chemical Reagent Co., Ltd. Trisodium citrate (99.0%) was purchased from Beijing Chemical Plant. All chemicals were used without further purification. Ultrapure water (18.2 MΩ) was used to make aqueous solutions.

**Instruments:** LEDs for homemade cylinder arrays (478, 503, 523 and 590 nm) were purchased from Shenzhen BYT Opto-electricity Co., Ltd. A temperature-controlled water-filled tank is designed and implemented to control the reaction temperature from 5 to 50 °C, in which a constant-temperature cycle device was purchased from Nanjing Xian'ou Instrument Manufacturing Co., Ltd. A UV–vis spectrometer (200–800 nm, CHEMUSB4000-UV/vis, Ocean Optics Inc.) was used to detect and monitor the evolution of the spectra during the photochemical growth process. Transmission electron microscope (TEM) images were taken with a Tecnai F20 instrument (FEI Co., Japan).

**Sample Preparation:** For preparation of silver seeds, ultrapure water (88 mL), AgNO3 (1 mL, 10 mM), and sodium citrate (10 mL, 10 mM) were combined in a 250 mL flask that immersed in an ice bath and stirred for 30 min. Aqueous $NaBH_4$ (0.8 mL, 10 mM, freshly prepared with ice-cold ultrapure water prior to injection) was added drop-wise into the mixture over the next 4 min. The resulting Ag colloid was rapidly stirred for 2 min in an ice bath. The reaction solution turned from colorless to bright yellow, which is the typical color for spherical nanoparticle silver colloids. These silver colloids exhibit an absorbance band at 400 nm. The bright yellow solution was then immediately exposed to LEDs. The reaction temperature was controlled at 5, 10, 20, 30, and 40 °C by a cycling device that maintained a constant temperature during the photomediated synthesis.

## Conclusions

Based on the results described above, we conclude that the combination of irradiation wavelength and reaction temperature controls the nanocrystal growth pathway and final nanoparticle morphology. A two-step process mechanism has been proposed. The primary process occurs when the silver nanoparticles absorb photons and enter short lived excited states generated by excitation of plasmon transitions. The secondary process consists of a series of thermal chemical reactions that proceed after particles are provided the necessary excitation energy. The excitation energy is dependent on irradiation wavelength. Only at short wavelength is the energy

high enough to efficiently overcome the energy barrier for conversion of silver seed to decahedra. The kinetic process can be controlled by reaction temperature. Fast reaction rates favor the growth of nanoprisms by preferential Ag deposition on {110} facets, while slow deposition on {111} favor the growth of nanodecahedra. The essential ingredients in explaining the results are (1) prisms are kinetically favored, (2) decahedra are thermodynamically favored and importantly (3) prisms can be excited by irradiation to transform to decahedra. This work reveals the intimate relationship between silver nanodecahedra and nanoprisms and highlights the importance of reaction kinetics in shape controlled, nanocrystal synthesis.

## Acknowledgements

This work was financially supported by the National Natural Science Foundation of China (No. 21275064, 21075051), Program for New Century Excellent Talents in University (NCET-10-0433), the fund of the State Key Laboratory of Advanced Technologies for Comprehensive Utilization of Platinum Metals (SKL-SPM-201207), the Fundamental Research Funds for the Jilin University (Grant No. 200903020), the "211" and "985" project of Jilin University, China. Work at ORNL was supported by the Department of Energy, Basic Energy Sciences, Materials Sciences and Technology Division.

## Notes and references

[a] Key Laboratory of Automobile Materials of MOE and State Key Laboratory of Superhard Materials, Department of Materials Science, Jilin University, Changchun 130012, People's Republic of China. E-mail: xqcui@jlu.edu.cn (X. C.), wtzheng@jlu.edu.cn (W.Z.)

[b] State Key Laboratory of Advanced Technologies for Comprehensive Utilization of Platinum Metals, Kunming, 650106, People's Republic of China.

[c] Materials Science and Technology Division, Oak Ridge National Laboratory, Oak Ridge, TN 37831-6056

Electronic Supplementary Information (ESI) available: [details of any supplementary information available should be included here]. See DOI: 10.1039/b000000x/

1 M. R. Langille; M. L. Personick; C. A. Mirkin, Angew. Chem. Int. Ed. 2013, 52, 13910-13940.
2 J. E. Millstone; S. J. Hurst; G. S. Metraux; J. I. Cutler; C. A. Mirkin, Small 2009, 5, 646-664.
3 X. Xia; J. Zeng; Q. Zhang; C. H. Moran; Y. Xia, J. Phys. Chem. C 2012, 116, 21647-21656.
4 X. Lu; M. Rycenga; S. E. Skrabalak; B. Wiley; Y. Xia, Annu. Rev. Phys. Chem. 2009, 60, 167-192.
5 R. C.Jin ; Cao Y. W.; Chad A. Mirkin; K. L. Kelly; George C. Schatz; J. G. Zheng, Science 2001, 294, 1901-1903.
6 R. C. Jin ; Cao Y. W.; Encai Hao; Gabriella S. Me´ traux; G. C. Schatz; C. A. Mirkin, Nature 2003, 425, 487-490.
7 Anne-Isabelle Henry; Julia M. Bingham; Emilie Ringe; Laurence D. Marks; George C. Schatz; R. P. V. Duyne, J. Phys. Chem. C 2011, 115, 9291–9305.
8 Andrea R. Tao; Susan Habas; P. Yang, Small 2008, 4, 310 – 325.
9 T. K. Sau; A. L. Rogach, Adv. Mater. 2010, 22, 1781-1804.
10 T. Mitsudome; Y. Mikami; M. Matoba; T. Mizugaki; K. Jitsukawa; K. Kaneda, Angew. Chem. Int. Ed. 2012, 51, 136-139.
11 P. Hervés; M. Pérez-Lorenzo; L. M. Liz-Marzán; J. Dzubiella; Y. Lu; M. Ballauff, Chem. Soc. Rev. 2012, 41, 5569–5868.
12 Amanda J. Haes; Shengli Zou; George C. Schatz; R. P. V. Duyne, J. Phys. Chem. B 2004, 108, 6961-6968.
13 Yi Wang; Dehui Wan; Shuifen Xie; Xiaohu Xia; Cheng Zhi Huang; Y. Xia, ACS Nano 2013, 7, 4586–4594.
14 J. Liu; X. Ren; X. Meng; Z. Fang; F. Tang, Nanoscale 2013, 5, 10022–10028.
15 X. Q. Cui; K. Tawa; K. Kintaka; J. Nishii, Adv. Funct. Mater. 2010, 20, 945-950.
16 Y. Wang; L. Chen; P. Liu, Chem.- Eur. J. 2012, 18, 5935-5943.
17 Y. Zhang; Y. Guo; Y. Xianyu; W. Chen; Y. Zhao; X. Jiang, Adv. Mater. 2013, 25, 3802–3819.
18 S. Cui; H. Pu; E. C. Mattson; G. Lu; S. Mao; M. Weinert; C. J. Hirschmugl; M. Gajdardziska-Josifovska; J. Chen, Nanoscale 2012, 4, 5887–5894.
19 M. Rycenga; C. M. Cobley; J. Zeng; W. Li; C. H. Moran; Q. Zhang; D. Qin; Y. Xia, Chem. Rev. 2011, 111, 3669-3712.
20 M. Rycenga; M. R. Langille; M. L. Personick; T. Ozel; C. A. Mirkin, Nano Lett. 2012, 12, 6218–6222.
21 S. M. Stranahan; E. J. Titus; K. A. Willets, J. Phys. Chem. Lett. 2011, 2, 2711-2715.
22 M. L. Personick; M. R. Langille; J. Zhang; J. Wu; S. Li; C. A. Mirkin, Small 2013, 9, 1947-1953.
23 G. Lu; H. Li; S. Wu; P. Chen; H. Zhang, Nanoscale 2012, 4, 860–863.
24 J. Zhang; S. Li; J. Wu; G. C. Schatz; C. A. Mirkin, Angew. Chem. Int. Ed. 2009, 48, 7787-7791.
25 M. R. Langille; J. Zhang; M. L. Personick; S. Li; C. A. Mirkin, Science 2012, 337, 954-957.
26 C. Xue; G. S. Metraux; J. E. Millstone; C. A. Mirkin, J. Am. Chem. Soc. 2008, 130, 8337-8344.
27 George P. Lee; Yichao Shi; Ellen Lavoie; Torben Daeneke; Philipp Reineck; Ute B. Cappel; David M. Huang; U. Bach, ACS Nano 2013, 7, 5911-5921.
28 K. G. S. a. J. C. Scaiano, J Am Chem Soc 2010, 132, 1825–1827.
29 J. Zhou; J. An; B. Tang; S. Xu; Y. Cao; B. Zhao; W. Xu; J. Chang; J. R. Lombardi, Langmuir 2008, 24, 10407-10413.
30 C. Xue; C. A. Mirkin, Angew. Chem. Int. Ed. 2007, 46, 2036-2038.
31 H. Wang; X. Zheng; J. Chen; D. Wang; Q. Wang; T. Xue; C. Liu; Z. Jin; X. Cui; W. Zheng, J. Phys. Chem. C 2012, 116, 24268-24273.
32 X. L. Zheng; X. J. Zhao; D. W. Guo; B. Tang; S. P. Xu; B. Zhao; W. Q. Xu; J. R. Lombardi, Langmuir 2009, 25, 3802-3807.
33 J. C. Scaiano; K. Stamplecoskie, J. Phys. Chem. Lett. 2013, 4, 1177-1187.
34 J. Zhang; S. Li; J. Wu; G. C. Schatz; C. A. Mirkin, Angew. Chem. Int. Ed. 2009, 48, 7787-7791.
35 X. L. Zheng; W. Q. Xu; C. Corredor; S. P. Xu; J. An; B. Zhao; J. R. Lombardi, J. Phys. Chem. C 2007, 111, 14962-14967.
36 A. Callegari; D. Tonti; Chergui, M., Nano Lett 2003, 3, 1565-1568.
37 Kuo, C. L.; Hwang, K. C., Chem. Mater. 2013, 25, 365-371.

38 B. Tang; J. An; X. L. Zheng; S. P. Xu; D. M. Li; J. Zhou; B. Zhao; W. Q. Xu, J. Phys. Chem. C 2008, 112, 18361-18367.
39 C. Xue; G. S. Metraux; J. E. Millstone; C. A. Mirkin, J Am Chem Soc 2008, 130, 8337-8344.
40 Y. Xia; Y. Xiong; B. Lim; S. E. Skrabalak, Angew. Chem. Int. Ed. 2008, 48, 60-103.
41 B. Pietrobon; V. Kitaev, Chem. Mater. 2008, 20, 5186-5190.
42 X. Xia; S. Xie; M. Liu; H. C. Peng; N. Lu; J. Wang; M. J. Kim; Y. Xia, Proc. Natl. Acad. Sci. U.S.A. 2013, 110, 6669-6673.

# Table of Contents